

## Research Article

# Factors Influencing the Rheological Properties of MRSP Based on the Orthogonal Experimental Design and the Impact Energy Test

Bing Liu,<sup>1,2</sup> Chengbin Du ,<sup>1</sup> and Yankai Fu<sup>1</sup>

<sup>1</sup>College of Mechanics and Materials, Hohai University, Nanjing 210098, China

<sup>2</sup>College of Civil Engineering, Wanjiang University of Technology, Ma'anshan 243031, China

Correspondence should be addressed to Chengbin Du; [cbdu@hhu.edu.cn](mailto:cbdu@hhu.edu.cn)

Received 3 July 2019; Accepted 29 July 2019; Published 22 September 2019

Academic Editor: Pramod Koshy

Copyright © 2019 Bing Liu et al. This is an open access article distributed under the Creative Commons Attribution License, which permits unrestricted use, distribution, and reproduction in any medium, provided the original work is properly cited.

In the preparation process of magnetorheological silly putty (MRSP), the influence factors of the relative shear thickening effect (RSE) and relative magnetorheological effect (RME) were studied by orthogonal experiments as well as range and variance analyses. The influence degree of each factor was also evaluated. The results showed that the viscosity of polydimethylsiloxane (PDMS) and the mass fraction of carbonyl iron powder (CIP) had a significant influence on the RSE and RME, respectively. With an increasing PDMS viscosity, the RSE of the silicon-boron copolymer matrix first increased and then decreased, while the RME of MRSP decreased gradually. In addition, the shear thickening mechanism of MRSP was explored by the molecular chain motion. Finally, the impact energy with different samples was tested, and it is demonstrated that with the increasing cross section, the impact energy of the sample increases gradually, but the rate of increase becomes smaller.

## 1. Introduction

Magnetorheological silly putty (MRSP), formed by uniformly dispersing micron-sized soft magnetic particles into a silicon-boron copolymer matrix, is a new type of intelligent material with both shear thickening and magnetorheological effects. Shear thickening (ST) phenomenon is a reversible non-Newtonian behavior. The viscosity of ST materials will change dramatically at a high-speed impact or extrusion, and when the force is removed, it transforms back to the initial state [1–3]. ST materials could passively respond to external load stimuli, helping important structures to achieve their self-adaptive and self-strengthening functions. Due to the rate-dependent properties, ST materials have been widely used in body armor, vibration control, and damping [4–8]. Recently, the most common ST materials are ST fluids (STFs) and ST gels (STGs). Under a magnetic field, materials with magnetorheological (MR) effect will change rapidly in milliseconds with an enormous and continuous reversibility. Compared with traditional materials, MR materials exhibit controllable stiffness and damping [9].

As liquid is used as the carrier, STF has lower mechanical properties and difficult encapsulation problems, so STG has gradually attracted growing research interests in the past decades [10, 11]. Dow Corning Corporation produces a rate-sensitive expansion compound (similar to plasticine) that can adjust the softness of materials by adding solid particles. Internationally, this material is commonly known as silly putty or SP for short. When the speed of the external force is fast, the SP will become harder. In contrast, when the speed of the external force is slow, the SP will become softer. The SP with carbonyl iron powder (CIP) is referred to as MRSP. The Cambridge Polymer Group [12] prepared SP on the basis of the formula of Dow Corning Co., proposing that the Deborah number (the ratio between the relaxation time and observation time) can reflect the viscoelasticity of materials. Golinelli et al. [13] studied the viscoelastic and magnetorheological behaviour of commercial magnetic silly putty. Xu et al. [14] selected SP-CaCO<sub>3</sub> as the sandwich and two layers of Kevlar as the panel to prepare a Kevlar/SP/Kevlar sandwich composite material using a mechanical method. In addition, the changing rule of the SP-CaCO<sub>3</sub> storage

modulus with frequency with different  $\text{CaCO}_3$  contents was tested by a rheometer. Martin et al. [15] found that mixing urea polyurethane with SP could improve the tensile strength of the SP and studied the loss modulus of this composite with a change in the angular frequency from 0.1 to 100 rad/s. Jiang et al. [16] dispersed  $\text{CaCO}_3$  particles into SP to obtain a buffer material with excellent performance and tested its performance via the drop-hammer test and Hopkinson bar technique. Boland et al. [17] dispersed nanosized graphene into SP, obtaining ultrasensitive electromechanical materials, which were used to capture the climbing signals of spiders. A multifunctional composite with both shear thickening and magnetorheological effects was gained by adding CIP into SP by Wang et al. [18]. Goertz et al. [19] investigated the influence of temperature on the rheological properties of SP and demonstrated that it varies significantly with temperature. Lin et al. [20] designed a novel shear thickening magnetorheological (STMR) damper with both locking and semiactive controlling properties and fabricated the damper based on multifunctional composite materials, defined as MRSP.

The mechanism of shear thickening phenomenon has also been extensively explored in recent years. Liu et al. [21] synthesized a silicon-boron copolymer at  $200^\circ\text{C}$  and analysed the bonds of B-O-B, B-O-H, and Si-O-B formed during the reaction process of polydimethylsiloxane (PDMS) and boric acid by using Fourier-transform infrared spectroscopy (FTIR). The findings indirectly proved the chemical process of PDMS dehydration polymerization with boric acid after chain fracture. Wang et al. [22] observed that in an SP-reinforced composite, the SP can effectively weaken the external force in the knee protection test due to the B-O bond. Cross [23] established a three-parameter viscoelastic mechanical model of SP and studied its mechanical properties under low and high strain rates. Furthermore, Wang et al. [24, 25] prepared a new kind of shear thickening gel (STG) and found that its shear thickening mechanism was in line with chemical bond theory.

At present, research studies on the rheological properties of MRSP have mainly focused on the influence of a single factor [16–19]. However, during the actual preparation process, many factors are involved. If all the factors are tested, the scale of the experiment would be large, and the efficiency would be relatively low. The orthogonal experimental design is a method that analyses multifactors and multilevels, which was put forward by British scholar Fisher. Fisher established the theory of “experimental design,” thereafter solving the problem of uneven experimental conditions. In the early 1950s, the Japanese quality management expert Dr. Genichi Taguchi proposed the “orthogonal experimental design” and discussed and optimized dozens of eigenvalues and more than 2000 experimental factors of a linear spring relay, a product of the Japan Institute of Telecommunications. Lee et al. [26] optimized and analysed the truss structure, insisting that orthogonal experimental design was obviously superior to the genetic algorithm in terms of the calculation time. With a deepening of the research on orthogonal experiments, many scholars at home and abroad have applied this

method to the pharmacological, industrial, agricultural production, food processing, and engineering technology fields [27].

In this paper, MRSP with a storage modulus increase of 3 orders of magnitude and a relative magnetorheological effect (RME) reaching more than 250% was prepared by dispersing CIP into the matrix of a silicon-boron copolymer with shear thickening properties. On the one hand, via orthogonal experiments, the quality and viscosity of PDMS, quality of pyroboric acid and absolute ethyl alcohol, heating time, and temperature that affect the shear thickening effect were discussed by an analysis of the range and variance. On the other hand, the qualities of the matrix mass, CIP, dicumyl peroxide (DCP) and glycerine, vulcanization time, and temperature affecting the magnetorheological effect were investigated. Meanwhile, the influence degree of the factors mentioned above was identified and the influence of the PDMS viscosity on the rheological properties was investigated. The shear thickening mechanism was also explored by the molecular chain motion. Finally, various samples of different sizes were prepared and the impact energy was tested.

## 2. Experimental Section

**2.1. Preparation of MRSP.** In this experiment, silicon-boron copolymer was used as the matrix, which consists of boric acid, PDMS, and absolute ethyl alcohol. In addition, the experimental materials also included the plasticizer glycerine, the cross-linked agent DCP, and CIP (Jiangsu Tianyi Ultra-Fine Metal Powder Co., Ltd., Xuyi, China) with an average particle size of  $3.5\ \mu\text{m}$ . The performance indexes of CIP are shown in Table 1. All the above materials were analytically pure and were purchased from Sinopharm Chemical Reagent Co., Ltd., Shanghai, China, except for the CIP. The rheological property was tested with an MCR series rheometer (Anton Paar Co., Austria).

The preparation process of MRSP is as follows:

- (1) A certain amount of boric acid was weighed and placed into a vacuum drying oven. The sample was continuously heated for 90 min at  $160^\circ\text{C}$ , and pyroboric acid was obtained.
- (2) Pyroboric acid, absolute ethyl alcohol, and PDMS with a viscosity of  $100\ \text{mm}^2/\text{s}$  were mixed. After stirring for 15 min, the mixture was placed in the vacuum drying oven. After heating for 600 min at  $230^\circ\text{C}$ , the silicon-boron copolymer, namely, the matrix with a shear thickening effect, was obtained after cooling.
- (3) The silicon-boron copolymer, CIP, DCP, and glycerine were mixed together in a certain proportion and stirred again for 15 min.
- (4) The mixture was placed in an oven and was vulcanized at  $125^\circ\text{C}$  for 60 min and then stirred for 15 min. After cooling, the MRSP samples were obtained.

The MRSP sample, scanning electron microscopy (SEM) and FTIR are shown in Figure 1.

TABLE 1: The major performance indexes of CIP.

Fe content	C content	O content	N content	Average particle size	Apparent density	Tap density
98.030%	0.730%	0.276%	0.964%	3.500 $\mu\text{m}$	2.800 $\text{g}\cdot\text{cm}^{-3}$	4.200 $\text{g}\cdot\text{cm}^{-3}$

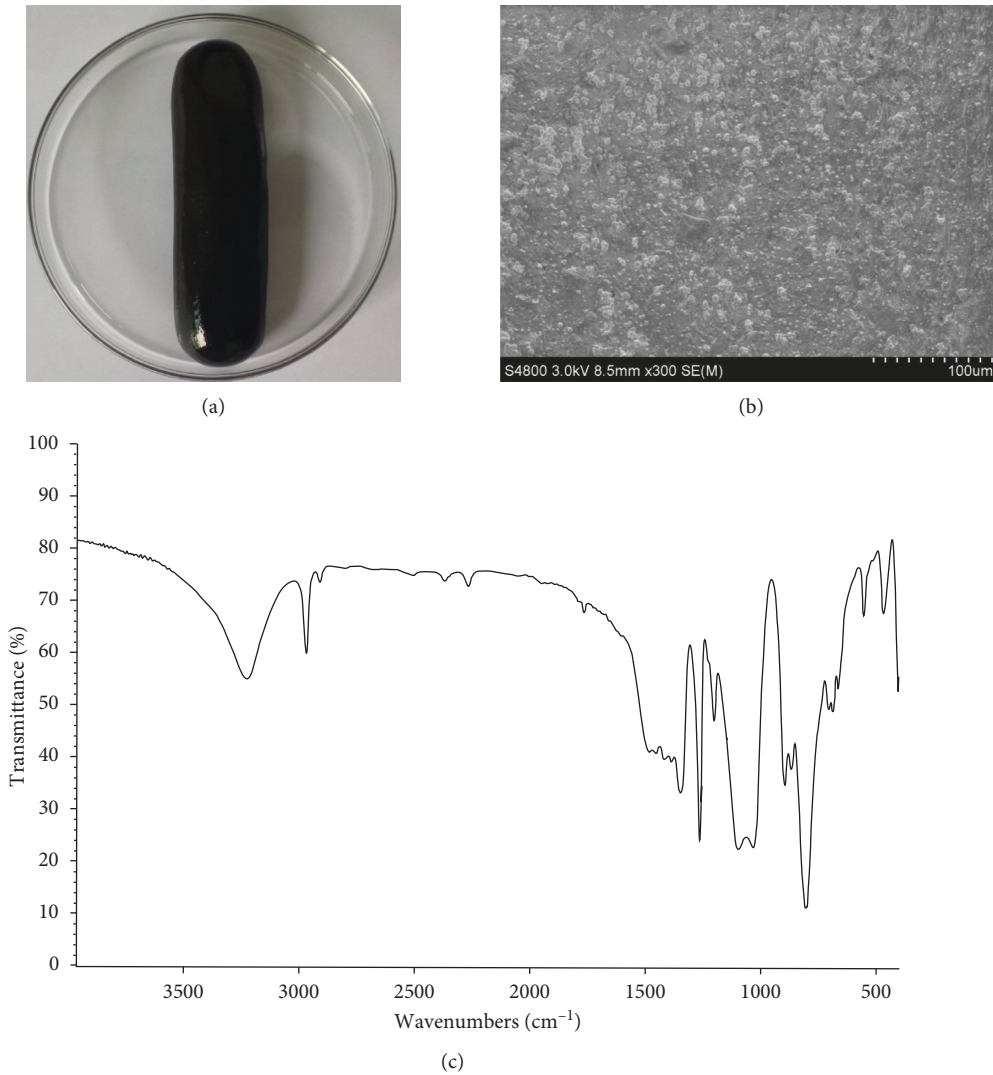


FIGURE 1: (a) The MRSP sample at a room temperature, (b) SEM image of the internal microstructure, and (c) FTIR spectrum in the range of 4000–500  $\text{cm}^{-1}$ .

The MRSP sample is like dough at a room temperature, as in Figure 1(a). Figure 1(b) shows the SEM image taken by a Hitachi S4800 scanning electron microscope. It can be seen that the CIP is uniformly dispersed in the matrix. Figure 1(c) shows the FTIR spectrum of the MRSP in the range of 4000–500  $\text{cm}^{-1}$ . The absorption peak at 2950  $\text{cm}^{-1}$  is due to the methyl asymmetric stretching. And the peak at 1350  $\text{cm}^{-1}$  is ascribed to the B-O vibration. The characteristic band of 1100  $\text{cm}^{-1}$  indicates the presence of the Si-O bond. In addition, the peaks at 890  $\text{cm}^{-1}$  and 860  $\text{cm}^{-1}$  relate to the Si-O-B bond, which proves the formation process of the MRSP and existence of cross-linked bonds.

Several kinds of raw materials and heating processes were involved during the preparation period, as shown in

Figure 2. Each heating process included the setting of the heating time and temperature. In consideration of the various influencing factors, the shear thickening and magnetorheological effects were explored by orthogonal experiments.

**2.2. Orthogonal Experimental Design.** Orthogonal experimental design is an important mathematical method to investigate multifactor tests, to select some representative tests according to orthogonality to achieve high efficiency, speed, and economy. This approach applies a standardized table (orthogonal table) to conduct experimental design and statistical analysis to discuss the results, thus revealing much

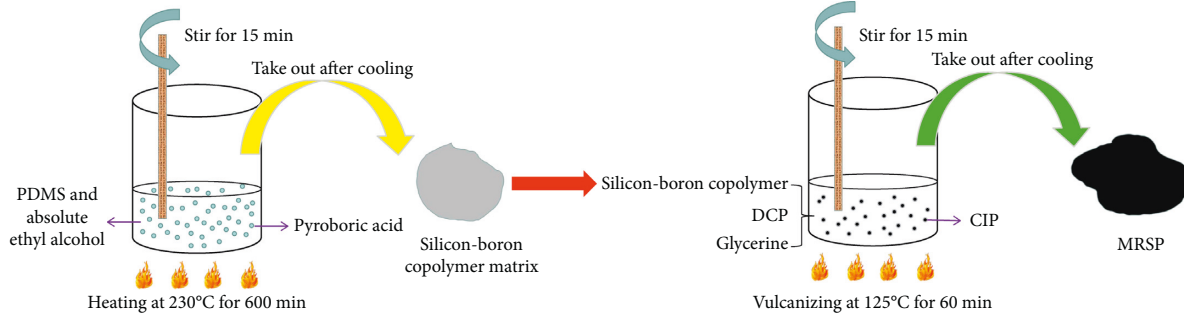


FIGURE 2: The operation process of silicon-boron copolymer and MRSP.

more accurate and reliable optimized conclusions with fewer trials.

In the preparation of a matrix with shear thickening properties, seven factors, namely, PDMS quality, PDMS viscosity, pyroboric acid quality, absolute ethyl alcohol quality, heating time, temperature and experimental error, were selected for the  $L_{18}(3^7)$  orthogonal test to study their influence on the shear thickening effect. Since the preparation method of pyroboric acid is relatively uniform, it is not necessary to set additional experimental factors in this process. “L” is the code of the orthogonal table, 18 represents the number of experiments, 3 represents the factor levels, indicating that each factor will be combined with 3 different values, and 7 is the number of factors considered in the experiment. In the preparation of MRSP, an  $L_{18}(3^7)$  orthogonal experiment was conducted on 7 factors, namely, the qualities of the matrix, CIP, DCP, glycerine, vulcanization time, temperature, and experimental errors, to study their influence on the magnetorheological effect. Then, the influencing degree of these factors were analysed and identified through a mathematical statistical method.

### 3. Results and Discussion

**3.1. Orthogonal Experimental Results and the Analysis of the Range and Variance.** MRSP displays an obvious shear thickening performance at a room temperature, while after the application of an external magnetic field, the CIP particles are arranged in chains in the matrix along the direction of the magnetic induction lines, which can also exhibit magnetorheological properties. To compare the shear thickening and magnetorheological effects, the RSE and RME were used to evaluate the performance:

$$RSE = \frac{G'_{\max} - G'_{\min}}{G'_{\min}} \times 100\%, \quad (1)$$

where  $G'_{\max}$  is the maximum shear storage modulus excited by the loading frequency and  $G'_{\min}$  is the initial shear storage modulus.

$$RME = \frac{G_{\max} - G_{\min}}{G_{\min}} \times 100\%, \quad (2)$$

where  $G_{\max}$  is the maximum shear storage modulus at magnetic saturation and  $G_{\min}$  is the initial zero field shear storage modulus.

The formula of the MRSP sample was employed as the benchmark, and the value itself and the values above 10% and below 10% were taken as the three levels other than the PDMS viscosity. The PDMS used in this study was purchased from Sinopharm Chemical Reagent Co., Ltd., and was divided into five categories according to its viscosity, namely, 50, 100, 350, 500, and 1000  $\text{mm}^2/\text{s}$ . In addition to the viscosity value of 100  $\text{mm}^2/\text{s}$  used in the sample, the upper and lower viscosity grades, namely, 50 and 350  $\text{mm}^2/\text{s}$ , were considered the three levels for research. The orthogonal table of RSE is shown in Table 2. In this table, 18 groups of experiments are tested.

Range analysis and variance analysis are common data processing methods used in orthogonal experiments. Range analysis is also called intuitive analysis, which is used to calculate the average range of each factor for data processing. This analysis estimates the difference between the maximum and minimum mean values of the test indexes under different levels. The greater the range of factors is, the larger the impact of the factor on the index is, so the more important the factor is. Through range analysis, the main factors affecting the indexes can be identified, and the optimal combination of factors can be found corresponding to the target eigenvalues. The results of the range analysis are shown in Figure 3.

Figure 3 shows the fluctuation and average RSE of each factor at different levels.  $A-k_i$  represents the average value of 6 experimental data at  $i$  level for factor A. Other factors are presented in the same way. The larger the ascending and descending amplitudes of the polyline graph are, the greater the influence of this factor on the RSE of the matrix is. The range value for each factor is shown in the bar graph, and obviously, the viscosity of PDMS has the most significant effect on the RSE.

Range analysis is simple and easy to understand. However, this method cannot distinguish the data fluctuations caused by changes in experimental conditions from those caused by experimental errors. In other words, this method cannot distinguish whether the differences in the experimental results are generated by factors or by test errors, and the experimental errors also cannot be estimated. In addition, it is impossible to give an accurate quantitative estimate of the effect of various factors on the test results and provide a standard to judge whether or not a certain factor is significant. Therefore, variance analysis can be applied to compensate for range analysis deficiencies.

TABLE 2: The orthogonal table of each factor on the RSE of the matrix.

Number	PDMS quality (g) (A)	PDMS viscosity (mm <sup>2</sup> /s) (B)	Pyroboric acid quality (g) (C)	Various factors absolute ethyl alcohol quality (g) (D)	Heating time (min) (E)	Heating temperature (°C) (F)	Error (G)
1	79.20	50	9.54	7.02	540	207	1
2	79.20	100	10.60	7.80	600	230	2
3	79.20	350	11.66	8.58	660	253	3
4	88.00	50	9.54	7.80	600	253	3
5	88.00	100	10.60	8.58	660	207	1
6	88.00	350	11.66	7.02	540	230	2
7	96.80	50	10.60	7.02	660	230	3
8	96.80	100	11.66	7.80	540	253	1
9	96.80	350	9.54	8.58	600	207	2
10	79.20	50	11.66	8.58	600	230	1
11	79.20	100	9.54	7.02	660	253	2
12	79.20	350	10.60	7.80	540	207	3
13	88.00	50	10.60	8.58	540	253	2
14	88.00	100	11.66	7.02	600	207	3
15	88.00	350	9.54	7.80	660	230	1
16	96.80	50	11.66	7.80	660	207	2
17	96.80	100	9.54	8.58	540	230	3
18	96.80	350	10.60	7.02	600	253	1

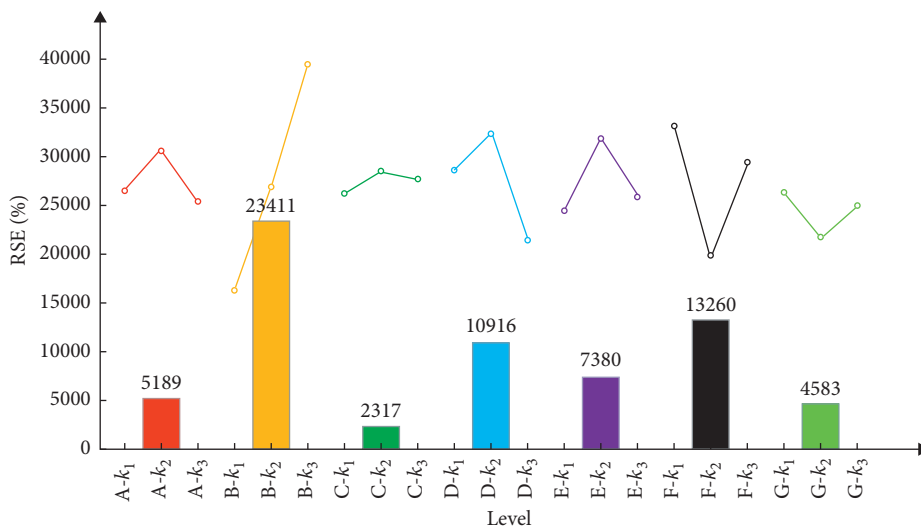


FIGURE 3: The average RSE of each factor under different levels.

The basic concept of variance analysis is to decompose the sum of the square of the deviations into two parts: the deviations caused by factors and those caused by errors. Then, the mean square of deviations is calculated and compared to determine the influence degree of each factor. Through the construction of statistics and the *F*-test, the significance of factors can be further identified. The specific calculation steps of the variance analysis are as follows:

- (1) Decompose the sum of the square of the deviations. The sum of the square of deviations equals the square of the deviations of each factor plus that of the errors:  $SS_T = SS_{\text{factor}} + SS_{\text{error}}$ .
- (2) Decompose the freedom degree:  $df_T = df_{\text{factor}} + df_{\text{error}}$ .

- (3) Calculate the variance:  $MS_{\text{factor}} = SS_{\text{factor}}/df_{\text{factor}}$ ,  $MS_{\text{error}} = SS_{\text{error}}/df_{\text{error}}$ .
- (4) Construct the *F*-statistics:  $F_{\text{factor}} = MS_{\text{factor}}/MS_{\text{error}}$ .
- (5) Prepare the variance table for *F*-test.

The *F*-test, also known as the test for the homogeneity of variance, is generally applied to examine the significance of the difference between the mean values of two or more random variables. In the *F* table,  $f_1$  represents the freedom degree of the numerator in the *F* value, while  $f_2$  stands for the freedom degree of the denominator, and the intersection is the critical value. The results of the *F*-test at different  $\alpha$  values and methods of presentation are shown in Table 3.

In the *F* distribution table, the thresholds of  $\alpha$  (0.01, 0.05, 0.10, and 0.25) correspond to 99.3, 19.3, 9.29, and 3.31,

TABLE 3: The results of the  $F$ -test and the methods of presentation.

Discriminant	Results	Presentation methods
$F > F_{0.01}(f_1, f_2)$	Highly significant	**
$F_{0.01}(f_1, f_2) \geq F > F_{0.05}(f_1, f_2)$	Significant	*
$F_{0.05}(f_1, f_2) \geq F > F_{0.10}(f_1, f_2)$	Slightly significant	(*)
$F_{0.10}(f_1, f_2) \geq F > F_{0.25}(f_1, f_2)$	Not significant but has influence	[*]
$F \leq F_{0.25}(f_1, f_2)$	No influence	No mark

respectively. The larger the  $F$  value is, the more significant the influence of this factor on the target eigenvalue is. During the preparation of the matrix, the range analysis and variance analysis of the RSE are shown in Table 4.

In the preparation of a matrix, the influence degree varying from high to low is in the following sequence: B  $\rightarrow$  F  $\rightarrow$  D  $\rightarrow$  E  $\rightarrow$  A  $\rightarrow$  G  $\rightarrow$  C. To obtain a better RSE, the optimum combination A2B3C2D2E2F1 can be selected for formula and performance improvement. The influence of each factor on RME during the preparation of MRSP is shown in Table 5.

Obviously, except for the quality of CIP, other factors have no obvious influence on the RME in the preparation of MRSP.

**3.2. Influence of the PDMS Viscosity on the Rheological Performance.** The orthogonal experimental results indicate that the viscosity of PDMS has a significant influence on the RSE of the matrix. As we know, PDMS is a kind of polyorganosiloxane in a chain structure with different polymerization degrees. PDMS has an excellent shear stability and can absorb vibrations, preventing vibration propagation, and thus can be used as a vibration damping fluid. The performance advantages and molecular structure of PDMS are shown in Figure 4.

PDMS can be divided into five categories according to its viscosity: 50, 100, 350, 500, and 1000 mm<sup>2</sup>/s. To further explore its influence on rheological properties, this experiment merely changed the PDMS viscosity on the basis of the previous formula, and the results are shown in Figures 5(a) and 5(b). The changing orders of magnitude of the shear storage modulus are shown in Table 6.

The experimental results reveal that when the PDMS viscosity is low, the maximum value of the storage modulus is small, resulting in changes of only two orders of magnitude with the changing angular frequency from 0.1 to 100 rad/s. In contrast, at a higher PDMS viscosity, the storage modulus also changes by only two orders of magnitude due to the larger initial value of  $G'$ . When the PDMS viscosity is 100 or 350 mm<sup>2</sup>/s, the shear storage modulus of the silicon-boron copolymer matrix could be stabilized at 3 orders of magnitude from 10<sup>3</sup> Pa to 10<sup>6</sup> Pa. A higher order of magnitude storage modulus variation means a better RSE and adjustable ability. According to the mass ratio of the matrix to CIP 1 : 0.7, the RME of MRSP was tested under the continuous changing of the magnetic flux density from 0 to 1000 mT. The results indicate that due to the small initial storage modulus, the RME of MRSP is large when the PDMS viscosity is low. As the PDMS viscosity increases, the initial

zero field storage modulus increases significantly, leading to a rapid decrease in RME.

#### 4. Shear Thickening Mechanism

During the preparation process of MRSP, the transition from the liquid state to the colloidal state in the cooling process is similar to the jamming phenomenon in physics [28–30]. The polymer exerts liquid-like properties under conditions of a low shear rate and density of the system as well as a high temperature and a large stress. By increasing the shear rate, cooling, reducing the stress, and increasing the system density, the polymer can realize the transition from liquid to colloidal or even solid state, as shown in Figure 6.

As a material with the highest mass percentage in MRSP preparation, PDMS belongs to the most common linear polymer in the organosilicon polymers, and its molecular chain behaves with decent flexibility. The Si-O bond angle in the chain is easy to change, which makes the chains very flexible, and the generation of rate-sensitivity phenomena depends on the entanglement and the motion of molecular chains. At the same time, boric acid is a kind of white powdery crystal that is widely used in the glass and ceramic industries. When the pyroboric acid reacts with PDMS at high temperature, the Si-O bond in the PDMS molecular chain is prone to fracture, leading to the introduction of boron B into the chain to form a Si-O-B bond. The molecular chain doped with the B element can take on three forms [31], as shown in Figure 7.

The formation of this Si-O-B bond is due to the lack of  $p$  orbital electrons in the B atom, which will steal electrons from the O atom in Si-O; thus, B and O atoms are attracted to each other, forming cross-linked bonds. Therefore, MRSP can realize a liquid-colloidal-solid transition. In Figure 8(a), free slip can be promoted between the different molecular chains, and the Si-O bond itself is also easy to rotate. It is due to the excellent flexibility of the PDMS molecular chain, and under this condition, the polymer can behave as a liquid. In Figure 8(b), the B-O cross-linked bond is formed between different molecular chains, which leads to the inability of free slip between them. To some extent, the movement of an individual chain is limited. In this case, the polymer exhibits the colloidal properties. In Figure 8(c), the rotation of the Si-O bond in the molecular chain will be restricted; that is, the overall motion of the chains will be further restrained, and the whole molecular chain will be fixed in the matrix. Thus, the polymer exhibits a performance of the solid state.

For MRSP, the faster the shear rate is, the higher the degree of jamming between the different molecular chains is,

TABLE 4: The range analysis and variance analysis of the RSE.

Influence factor	PDMS quality (A)	PDMS viscosity (B)	Pyroboric acid quality (C)	Absolute ethyl alcohol quality (D)	Heating time (E)	Heating temperature (F)	Error (G)
Influence degree (high → low)	B → F → D → E → A → G → C						
Optimal combination	A2B3C2D2E2F1						
Significance level	No mark	(*)	No mark	No mark	No mark	[*]	No mark

TABLE 5: The range analysis and variance analysis of the RME.

Influence factor	Quality of silicon-boron copolymer (A)	CIP quality (B)	DCP quality (C)	Glycerine quality (D)	Vulcanization time (E)	Vulcanization temperature (F)	Error (G)
Influence degree (high → low)	B → E → C → D → F → A → G						
Optimal combination	A2B1C2D2E2F2						
Significance level	No mark	(*)	No mark	No mark	No mark	No mark	No mark

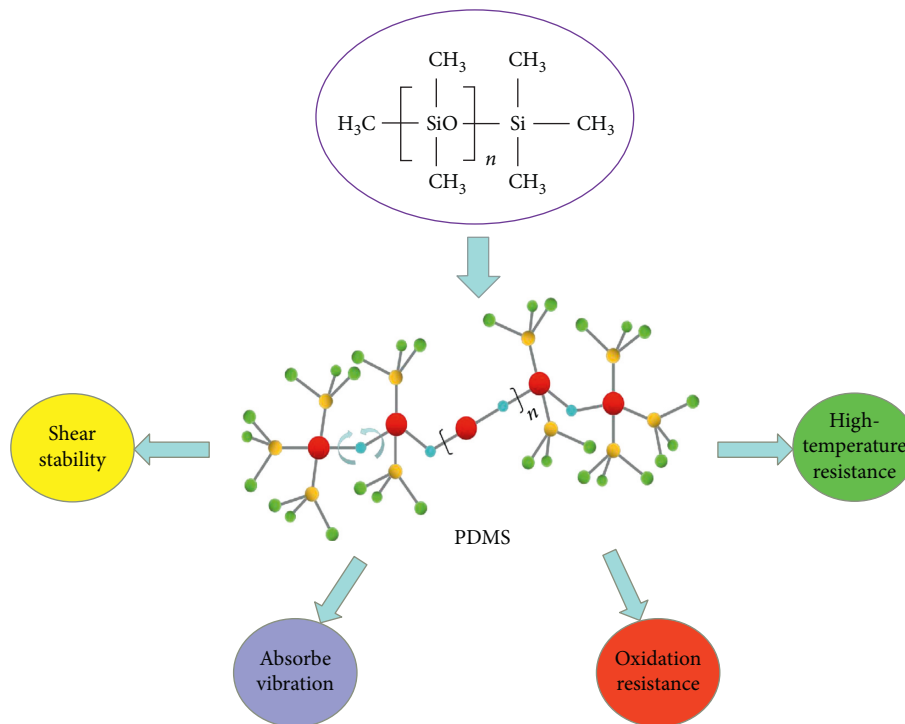


FIGURE 4: The performance advantages and molecular structure of PDMS.

and the closer the material is to a macroscopic solid. In contrast, the slower the shear rate is, the lower the degree of jamming is, and the closer the material is to a liquid state. In addition to the shear rate, the transition of tristate properties can be also achieved by changing the temperature, stress, and the system density.

### 5. Impact Energy Test

Due to the rate-sensitive properties, the silicon-boron copolymer will become hard to offset the rapid stimuli.

Therefore, five groups of sample are prepared and each group includes three samples with the same sizes. The samples are prone to change in shape, and a kind of solid fiberboard is chosen for the shape maintenance. And each group also contains an empty sample to test the impact energy of the solid fiberboard. The difference in the impact energy value between the sample and the solid fiberboard is the value for the silicon-boron copolymer matrix. The preparation process and the machine are shown in Figure 9.

The impact energy for each group and the change rules are shown in Figure 10. The results show that with the

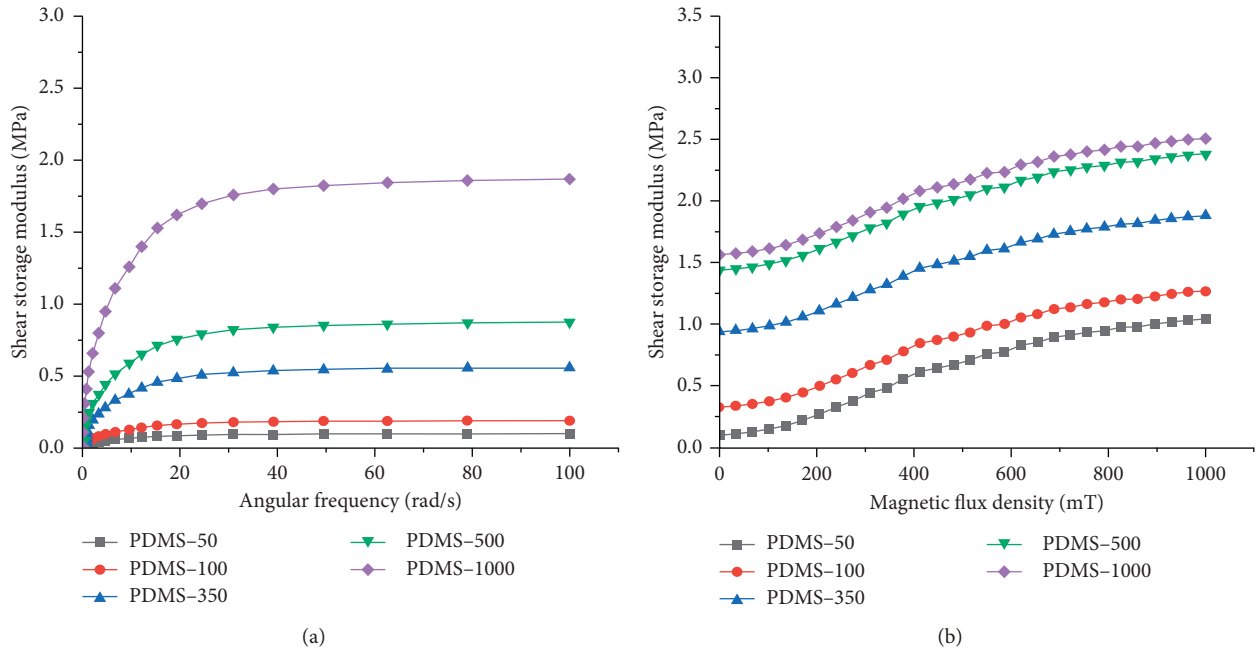


FIGURE 5: (a) The RSE of the continuously changing angular frequency from 0.1 to 100 rad/s and (b) the RME of the continuously changing magnetic flux density from 0 to 1000 mT with different PDMS viscosities.

TABLE 6: The changing orders of magnitude of the shear storage modulus with different PDMS viscosities.

PDMS viscosity	50	100	350	500	1000
Changing orders of magnitude of the MRSP shear storage modulus	2	3	3	2	2

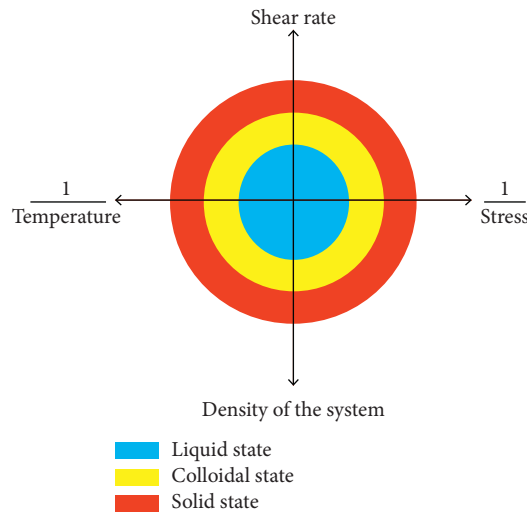


FIGURE 6: The phase change diagram and the influence factors of MRSP.

increasing cross section, the impact energy of these material increases gradually, but the rate of increase becomes smaller. If the cross section is 10 mm × 10 mm, the impact energy is less than 2J. When the size rises to 15 mm × 15 mm and 20 mm × 20 mm, the impact value has been greatly improved. Once the size is more than 20 mm × 20 mm, the impact energy grows more slowly. Among all the samples,

the highest average value of the impact energy reaches 11.8 J with the 30 mm × 30 mm cross-sectional size.

## 6. Conclusions

- (1) Through orthogonal experiments, the main factors affecting the shear thickening effect and

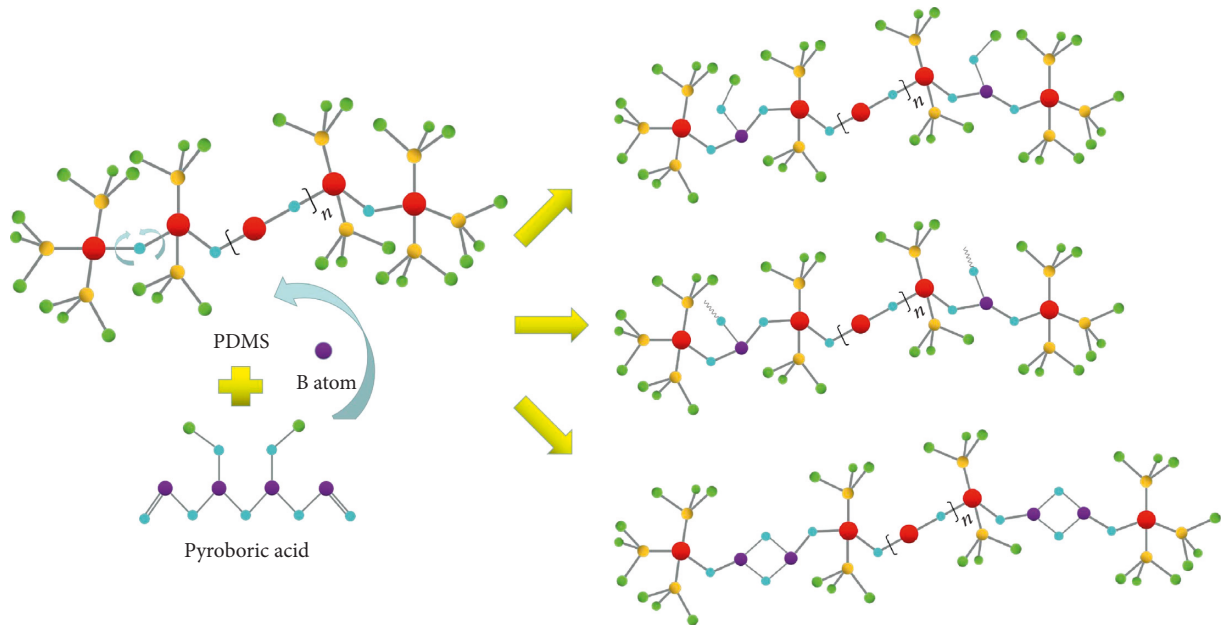


FIGURE 7: Three possible structural forms of the molecular chain doped with element B.

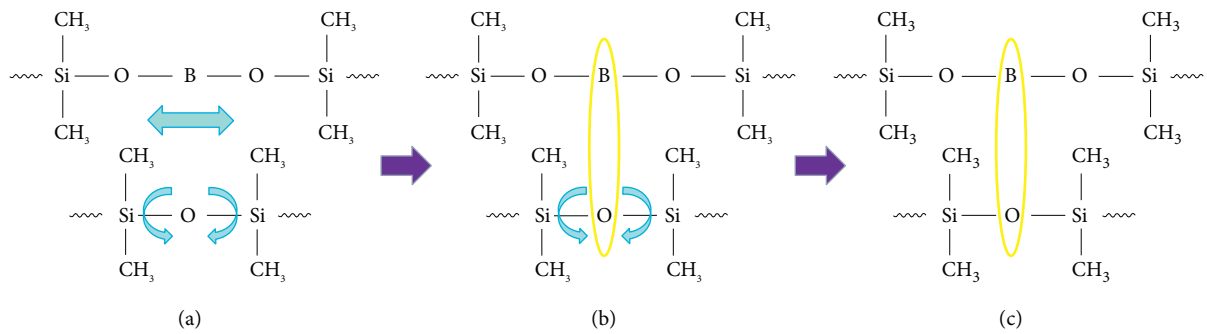


FIGURE 8: The movement mode of the internal molecular chains (a) when MRSP behaves as a liquid, (b) when MRSP behaves as a colloid, and (c) when MRSP behaves as a solid.

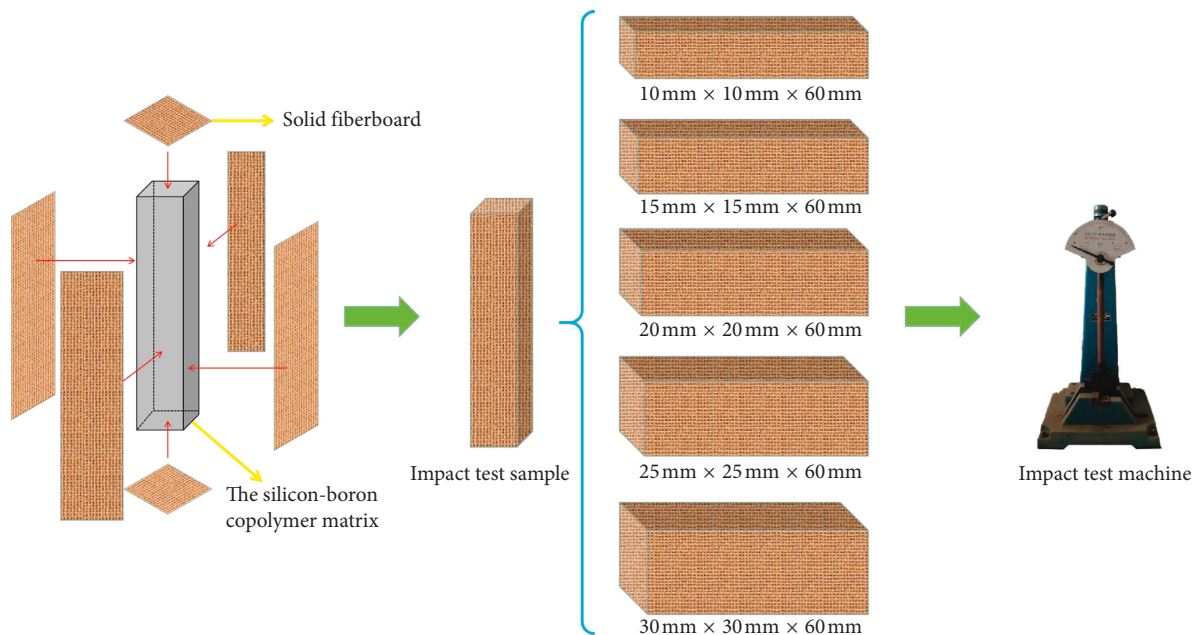


FIGURE 9: The preparation process of the test samples and the impact test machine.

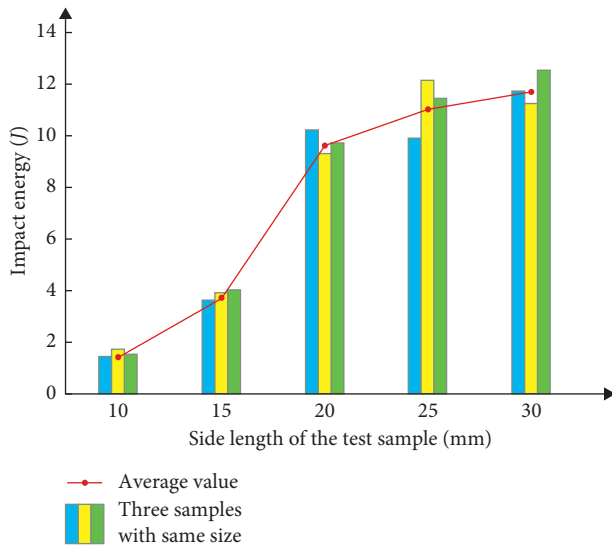


FIGURE 10: The impact energy for the sample in each group and the average values.

magnetorheological effect are explored using range and variance analyses in the matrix and MRSP preparations, and the influence degree of each factor is distinguished. The results reveal that the PDMS viscosity has the greatest impact on the shear thickening effect of the matrix. And during the preparation of MRSP, no other factors affect the magnetorheological effect except for CIP.

- (2) With increasing PDMS viscosity, the shear thickening effect of the matrix first increases and then decreases. When the PDMS viscosity is  $50 \text{ mm}^2/\text{s}$ ,  $500 \text{ mm}^2/\text{s}$ , and  $1000 \text{ mm}^2/\text{s}$ , its storage modulus changes by two orders of magnitude under the continuous changing angular frequency from 0.1 to 100 rad/s. This is due to the lower maximum shear storage modulus or higher initial modulus. When the PDMS viscosity is  $100 \text{ mm}^2/\text{s}$  or  $350 \text{ mm}^2/\text{s}$ , the storage modulus can increase by three orders of magnitude. With an increase in the PDMS viscosity, the RME of MRSP exhibits a decreasing trend.
- (3) The shear thickening effect is achieved by the generation and destruction of B-O cross-linked bonds and the motion of the molecular chains. Furthermore, on a macroscopic level, the shear rate is closely related to the state of the polymer. In addition to the shear rate, the temperature, stress, and system density can also realize the state transition of the MRSP.
- (4) The impact energy of the silicon-boron copolymer is tested. The impact energy grows fast if the size of the sample is less than  $20 \text{ mm} \times 20 \text{ mm}$ . When the cross-sectional size is more than it, the value will gradually stabilize. For the sample of  $10 \text{ mm} \times 10 \text{ mm}$ , the value is not more than 2 J. And the impact energy is approximately 11.8 J for the  $30 \text{ mm} \times 30 \text{ mm}$  sample.

## Data Availability

The data used to support the findings of this study are included within the article.

## Conflicts of Interest

The authors declare that there are no conflicts of interest regarding the publication of this paper.

## Acknowledgments

The authors gratefully acknowledge support from the Jiangsu Province Key R&D Project (grant no. BE2017167), the National Natural Science Foundation of China (grant no. 51579084), and the Fundamental Research Funds for the Central Universities (2018B48514).

## References

- [1] R. L. Hoffman, "Discontinuous and dilatant viscosity behavior in concentrated suspensions. II. Theory and experimental tests," *Journal of Colloid and Interface Science*, vol. 46, no. 3, pp. 491–506, 1974.
- [2] H. A. Barnes, "Shear-thickening ("Dilatancy") in suspensions of nonaggregating solid particles dispersed in Newtonian liquids," *Journal of Rheology*, vol. 33, no. 2, pp. 329–366, 1989.
- [3] E. Brown and H. M. Jaeger, "Shear thickening in concentrated suspensions: phenomenology, mechanisms and relations to jamming," *Reports on Progress in Physics*, vol. 77, no. 4, Article ID 046602, 2014.
- [4] Y. S. Lee, E. D. Wetzel, and N. J. Wagner, "The ballistic impact characteristics of Kevlar woven fabrics impregnated with a colloidal shear thickening fluid," *Journal of Materials Science*, vol. 38, no. 13, pp. 2825–2833, 2003.
- [5] X. Z. Zhang, W. H. Li, and X. L. Gong, "The rheology of shear thickening fluid (STF) and the dynamic performance of an STF-filled damper," *Smart Materials and Structures*, vol. 17, no. 3, Article ID 035027, 2008.
- [6] M. H. Wei, G. Hu, L. Jin, K. Lin, and D. Zou, "Forced vibration of a shear thickening fluid sandwich beam," *Smart Materials and Structures*, vol. 25, no. 5, Article ID 055041, 2016.
- [7] T. J. Kang, C. Y. Kim, and K. H. Hong, "Rheological behavior of concentrated silica suspension and its application to soft armor," *Journal of Applied Polymer Science*, vol. 124, no. 2, pp. 1534–1541, 2011.
- [8] T. F. Tian and M. Nakano, "Design and testing of a rotational brake with shear thickening fluids," *Smart Materials and Structures*, vol. 26, no. 3, Article ID 035038, 2017.
- [9] T. Shiga, A. Okada, and T. Kurauchi, "Magnetorheological behavior of composite gels," *Journal of Applied Polymer Science*, vol. 58, no. 4, pp. 787–792, 1995.
- [10] Q. He, S. Cao, Y. Wang, S. Xuan, P. Wang, and X. Gong, "Impact resistance of shear thickening fluid/Kevlar composite treated with shear-stiffening gel," *Composites Part A: Applied Science and Manufacturing*, vol. 106, pp. 82–90, 2018.
- [11] D. Y. Wu, S. Meure, and D. Solomon, "Self-healing polymeric materials: a review of recent developments," *Progress in Polymer Science*, vol. 33, no. 5, pp. 479–522, 2008.
- [12] Cambridge Polymer Group, "The Cambridge polymer group silly putty "Egg", 2002, [http://www.campoly.com/files/7213/9937/8983/CS\\_CPG\\_Silly\\_Putty\\_Egg\\_Rheology.pdf](http://www.campoly.com/files/7213/9937/8983/CS_CPG_Silly_Putty_Egg_Rheology.pdf).

- [13] N. Golinelli, A. Spaggiari, and E. Dragoni, "Mechanical behaviour of magnetic silly putty: viscoelastic and magnetorheological properties," *Journal of Intelligent Material Systems and Structures*, vol. 28, no. 8, pp. 953–960, 2015.
- [14] C. Xu, Y. Wang, J. Wu et al., "Anti-impact response of Kevlar sandwich structure with silly putty core," *Composites Science and Technology*, vol. 153, pp. 168–177, 2017.
- [15] R. Martin, A. Rekondo, A. Ruiz de Luzuriaga, A. Santamaria, and I. Odriozola, "Mixing the immiscible: blends of dynamic polymer networks," *RSC Advances*, vol. 5, no. 23, pp. 17514–17518, 2015.
- [16] W. F. Jiang, X. L. Gong, S. Wang et al., "Strain rate-induced phase transitions in an impact-hardening polymer composite," *Applied Physics Letters*, vol. 104, no. 12, Article ID 121915, 2014.
- [17] C. S. Boland, U. Khan, G. Ryan et al., "Sensitive electromechanical sensors using viscoelastic graphene-polymer nanocomposites," *Science*, vol. 354, no. 6317, pp. 1257–1260, 2016.
- [18] S. Wang, W. Jiang, W. Jiang et al., "Multifunctional polymer composite with excellent shear stiffening performance and magnetorheological effect," *Journal of Materials Chemistry C*, vol. 2, no. 34, pp. 7133–7140, 2014.
- [19] M. P. Goertz, X.-Y. Zhu, and J. E. Houston, "Temperature dependent relaxation of a "solid-liquid"," *Journal of Polymer Science Part B: Polymer Physics*, vol. 47, no. 13, pp. 1285–1290, 2009.
- [20] X. G. Lin, F. Guo, C. B. Du et al., "The mechanical properties of a novel STMR damper based on magnetorheological silly putty," *Advances in Materials Science and Engineering*, vol. 2018, Article ID 2681461, 15 pages, 2018.
- [21] Z. Liu, S. J. Picken, and N. A. M. Besseling, "Polyborosiloxanes (PBSs), synthetic kinetics, and characterization," *Macromolecules*, vol. 47, no. 14, pp. 4531–4537, 2014.
- [22] Y. Wang, S. Wang, C. Xu, S. Xuan, W. Jiang, and X. Gong, "Dynamic behavior of magnetically responsive shear-stiffening gel under high strain rate," *Composites Science and Technology*, vol. 127, pp. 169–176, 2016.
- [23] R. Cross, "Elastic and viscous properties of silly putty," *American Journal of Physics*, vol. 80, no. 10, pp. 870–875, 2012.
- [24] S. Wang, S. Xuan, W. Jiang et al., "Rate-dependent and self-healing conductive shear stiffening nanocomposite: a novel safe-guarding material with force sensitivity," *Journal of Materials Chemistry A*, vol. 3, no. 39, pp. 19790–19799, 2015.
- [25] S. Wang, S. Xuan, Y. Wang et al., "Stretchable polyurethane sponge scaffold strengthened shear stiffening polymer and its enhanced safeguarding performance," *ACS Applied Materials & Interfaces*, vol. 8, no. 7, pp. 4946–4954, 2016.
- [26] K.-H. Lee, J.-W. Yi, J.-S. Park, and G.-J. Park, "An optimization algorithm using orthogonal arrays in discrete design space for structures," *Finite Elements in Analysis and Design*, vol. 40, no. 1, pp. 121–135, 2003.
- [27] R. J. Liu, Y. W. Zhang, C. W. Wen, and J. Tang, "Study on the design and analysis methods of orthogonal experiment," *Experimental Technology and Management*, vol. 27, no. 9, pp. 52–55, 2010.
- [28] H.-N. Lee, K. Paeng, S. F. Swallen, and M. D. Ediger, "Direct measurement of molecular mobility in actively deformed polymer glasses," *Science*, vol. 323, no. 5911, pp. 231–234, 2009.
- [29] L. Berthier and G. Biroli, "Theoretical perspective on the glass transition and amorphous materials," *Reviews of Modern Physics*, vol. 83, no. 2, pp. 587–645, 2011.
- [30] A. Y. Malkin and V. G. Kulichikhin, "Shear thickening and dynamic glass transition of concentrated suspensions. State of the problem," *Colloid Journal*, vol. 78, no. 1, pp. 1–8, 2016.
- [31] T. I. Zatsepina, M. L. Brodskii, Y. A. Frolova, A. A. Trapeznikov, V. N. Gruber, and G. A. Kruglova, "Rheological behaviour of polyheterosiloxanes," *Polymer Science U.S.S.R.*, vol. 12, no. 11, pp. 2899–2905, 1970.



**Hindawi**  
Submit your manuscripts at  
[www.hindawi.com](http://www.hindawi.com)

